DOI: 10.6060/mhc224061i

Precursors for the Synthesis of Macroheterocyclic Compounds. Modeling of the Mechanism for Formation of 2–Amino–5–methyl–1,3,4–thiadiazole by Quantum Chemistry Methods

Yu. V. Suvorova, V. V. Dunaeva, and M. K. Islyaikin@

Ivanovo State University of Chemistry and Technology, Research Institute of Macroheterocycles, IRLoN, 153000 Ivanovo, Russia
@Corresponding author E-mail: islyaikin@isuct.ru

Dedicated to the memory of Prof. Geliy Vasilievich Ponomarev

The work presents 2-amino-5-methyl-1,3,4-thiadiazole formation simulation by DFT/B3LYP/6-31G(d,p), DFT/B3LYP/6-311+G(2d2p), MP2/6-311+G(2d2p) methods. It was established that the 2-amino-5-methyl-1,3,4-thiadiazole formation is a complicate multi-stage process that occurs through a number of elementary chemical transformations, the activation barriers of which were estimated.

Keywords: Aminothiadiazole, quantum chemistry calculation, density functional theory.

Прекурсоры синтеза макрогетероциклических соединений. Моделирование механизма образования 2–амино–5–метил–1,3,4–тиадиазола методами квантовой химии

Ю. В. Суворова, В. В. Дунаева, М. К. Исляйкин@

Ивановский государственный химико-технологический университет, НИИ Макрогетероциклических соединений, IRLoN, 153000 Иваново, Российская Федерация
@E-mail: islyaikin@isuct.ru

Посвящается памяти проф. Гелия Васильевича Пономарева

В работе представлено моделирование образования 2-амино-5-метил-1,3,4-тиадиазола методами DFT/B3LYP/6-31G(d,p), DFT/B3LYP/6-311+G(2d2p), MP2/6-311+G(2d2p). Было установлено, что образование 2-амино-5-метил-1,3,4-тиадиазола представляет собой сложный многостадийный процесс, который происходит через ряд элементарных химических превращений, барьеры активации которых были оценены.

Ключевые слова: Аминотиадиазол, квантово-химический расчет, теория функционала плотности.

Introduction

Substances bearing pharmacophore 1,3,4-thiadiazole groups are widely used as active components of various medical drugs such as Diacarb, Methazolamide, Ethazole, Tizanidine exhibiting anti-inflammatory, antimicrobial, antiviral, bronchodilator, antituberculosis and antitumor activities.[1–3]

Due to different structural modifications, such as amino groups transformation and introduction of substituents into heterocyclic core, 2,5-diamino-1,3,4-thiadiazole and its bi- and polynuclear derivatives are widely applied as precursors in the synthesis of various compounds.

Among the synthetic methods of the compounds bearing one or several 1,3,4-thiadiazole rings developed so far,[1–5] an oxidative condensation of dithiourea by hydrogen

peroxide is the most prevalent.[2,4,5] In order to synthesize binuclear amines consisting of two 1,3,4-thiadiazole residues united by alkyl bridges of various length, a condensation of corresponding dicarboxylic acids dichlorides with thiosemicarbazide in acid medium was used.[1]

Moreover, binuclear diamines corresponding to the general formula H_2N-R-X-R-NH_2 (where R is 1,3,4-thiadiazole ring) present a special interest as precursors of macroheterocyclic compounds (Mc) since their implementation into macrocyclic framework leads to the macrocyclic systems with expanded and well adjustable coordination cavities. By selection of diamines, it is possible to design a number of macrocycles with various coordination cavity,[6–10] which can be used as therapeutic agents for photodynamic therapy and virology,[11–12] nonlinear optical materials,[13] anion receptors,[14–17] and controlled drug release systems.[18]

An expanded AABAAB-type macroheterocycle (Figure 1A) was synthesized for the first time by the authors[19] using 4,4'-oxodianiline and 1,3-diiminoisoindoline as initial compounds. Its structure was confirmed by X-ray analysis.

In 1996 the authors[6] have obtained the similar six-membered Mc with thiadiazole subunits bounded *via* disulfide bridges (Figure 1B) by interaction of bis(5-amino-1,3,4-thiadiazole-2)disulfide and 1,3-diiminoisoindoline in alcohol medium. Due to presence of expanded coordination cavity including a number of heteroatoms, this Mc is able to coordinate the cations of large radius metals by selective and reversible way fashion. Therefore, it is recommended for purification of aqueous solutions from heavy metal ions such as strontium and lead.[20]

Cu complex of AAB'AAB'-type Mc (where B' is pyrrole ring bearing bulky substituents) (Figure 1C) was synthesized by condensation of 2,5-diamino-1,3,4-thiadiazole and 3,4-bis(4-*tert*-butyl)diiminopyrroline in boiling isopropanol using copper acetate as template in 2010.[21]

In 2016 the Mc of AABAAB-type with expanded coordination cavity was obtained by condensation of bis(5-amino-1,3,4-thiadiazole-2-yl)ethane (fragment A) and *tert*-butyldiiminoisoindoline (fragment B) (Figure 1D).[22]

It appears from the above materials, that structural diversity of macroheterocyclic compounds with expanded coordination cavity in comparison with enlarged phthalocyanine analogues[23] is essentially determined by the nature of parent binuclear diamines involved into crossover condensation with phthalogenes. Moreover, binuclear diamines such as bis(5-amino-1,2,4-triazole-3-yl)alkanes and bis(5-amino-1,3,4-thiadiazole-2-yl)alkanes have the greatest potential. The synthesis and properties of bistriazole alkanes were studied earlier.[24–27] The methods of obtaining of bis(5-amino-1,3,4-thiadiazole-2-yl)alkanes having antibacterial and antifungal properties also were claimed by the authors.[1] Despite its significant importance, formation mechanism of the latter remains unknown at the moment.

The authors[28] hypothesized that the 2,5-diamino-1,3,4-thiadiazole formation occurs due to an intramolecular nucleophilic attack of mercapto or amino group of dithiourea followed by elimination of hydrogen sulfide or ammonia molecules, respectively. However, any evidence of the proposed mechanism has not been published.

Taking into consideration that in the molecules of bis(5-amino-1,3,4-thiadiazole-2-yl)alkanes the 2-amino-1,3,4-thiadiazole subunits are separated by the alkyl groups and thereof a formation of each of heterocycles can be considered as the same independent process, the 2-amino-5-methyl-1,3,4-thiadiazole formation was accepted as a modeling one. In view of the foregoing, we have earlier published the preliminarily studies of a mechanism of 2-amino-5-methyl-1,3,4-thiadiazole formation using quantum chemistry methods.[29] It is worthy to note, that 2-amino-5-methyl-1,3,4-thiadiazole has practical importance itself.

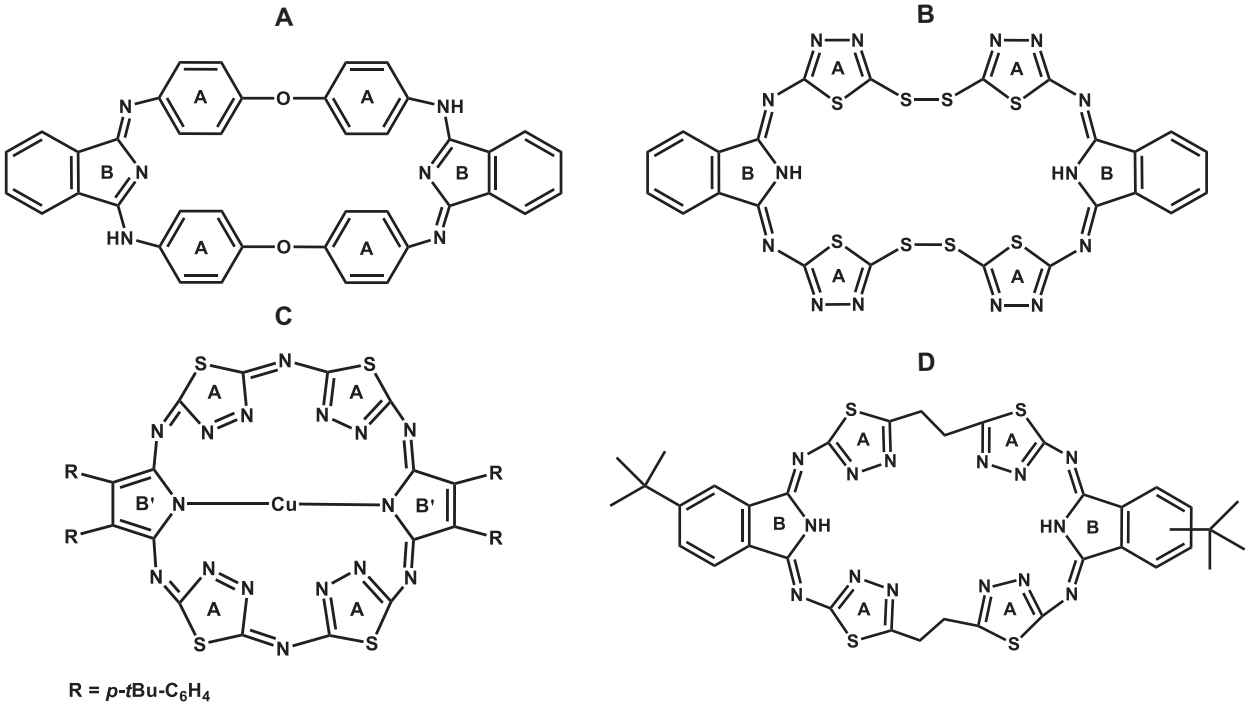

Figure 1. The structure of Mcs with expanded coordination cavity.

For example, the metal complexes of Mg(II), Zn(II), Mn(II), Cu(II), Co(II), Ni(II), Be(II), Cd(II), Pb(II), Al(III), Fe(III), and La(III) derived from 2-amino-5-methyl-1,3,4-thiadiazole and its derivatives behave as very powerful inhibitors against the three carbonic anhydrase isozymes.[30]

Thus, the aim of this work is 2-amino-5-methyl-1,3,4-thiadiazole formation simulation by quantum chemistry methods.

Computations

Quantum chemistry calculations of the reactants, transition states and products of all elementary stages which form full reaction pathway were carried out by DFT method using B3LYP hybrid functional (Becke + Slater + HF exchange and LYP + VWN5 correlation) and basis sets 6-31G(d,p) and 6-311+G(2d2p) as well as MP2/6-311+G(2d2p) computations. All calculations of protonated (q=1, M=1) and neutral (q=0, M=1) molecular forms were carried out using Firefly 8.2.0[31,32] software package with full geometry optimization without geometry constrains. Transition states (TSs) were found using SADPOINT procedure. Cartesian coordinates (Å) and total energy values (a.u.) of the structures optimized at the DFT/B3LYP/6-311+G(2d2p) and MP2/6-311+G(2d2p) levels are shown in Supporting Materials. Vibration frequencies performed in harmonic approximation show that the optimized structures as well as transition states are the corresponding critical points of the potential energy surfaces.[33] IRC subroutine was used to check each TSs on correspondence to the considered reaction pathway. Thermochemistry calculations were performed at various temperatures using Firefly 8.2.0.[31] Preparation of initial geometry, processing and obtained results visualization were performed using the ChemCraft program.[34]

Results and Discussion

Presumably, mechanism of 2-amino-5-methyl-1,3,4-thiadiazole formation can be represented as multisteps pathway (Scheme 1):

1. Tautomerism of thiosemicarbazide from thione-amino- (**1a**) to thioleimino- (**1b**) form.

2. The formation of protonated *N*-[(dihydroxymethyl)-methane]hydrazinoiminomethanethiole (**2a**) is carried out at interaction of protonated acetic acid molecule with thiosemicarbazide (**1b**);

3. Following dehydratation of **2a**, protonated *N*-[(hydroxymethyl)methane]hydrazinoiminomethanethiole (**2b**) is formed;

4. The cyclization and dehydratation of **2b** lead to protonated 2-imino-5-methyl-1,3,4-thiadiazoline (**3a**) formation;

5. Transformation of the protonated **3a** to **4** can go by two ways: tautomerism of **3a** and deprotonation of **3b**; or deprotonation of **3a** and tautomer transformation of **3c**.

At the first stage the calculations were performed at the DFT level using the most spread combination of hybrid functional B3LYP and basis set 6-31G(d,p). In order to increase the calculations accuracy, the enlarged basis 6-311+G(2d,2p) was applied since earlier it was successfully applied in S_E2 mechanism simulation.[35–37]

In the first step of the research, the thione- (**1a**)/thiole-(**1b**) tautomerism of thiosemicarbazide (Scheme 2) was studied. In results of both B3LYP/6-311+G(2d2p) and MP2/6-311+G(2d2p) calculations, the similar configurations have been achieved (see Supporting Materials).

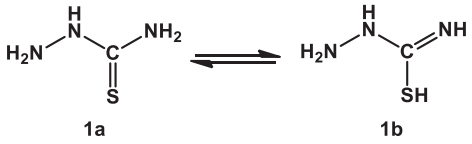

Scheme 2. Tautomeric forms of thiosemicarbazide molecule.

It was found that the hydrogen atom H1 is transferred between the nitrogen atom N3 of the amino group and sulfur S1 *via* the transition state **TS1**. Views of optimized configurations **1a**, **TS1**, and **1b** derived from calculations by DFT method using B3LYP hybrid functional and basis set 6-31G(d,p) are shown in Figure 2. The calculations by both B3LYP/6-311+G(2d2p) and MP2/6-311+G(2d2p) methods lead to similar configurations.

Following DFT calculations, amino/imino-tautomerism runs over an activation barrier, the value of which is decreased when enlarged basis set is used. Compared to the data, MP2 overestimates this characteristic. Such lack of accordance was described earlier.[38]

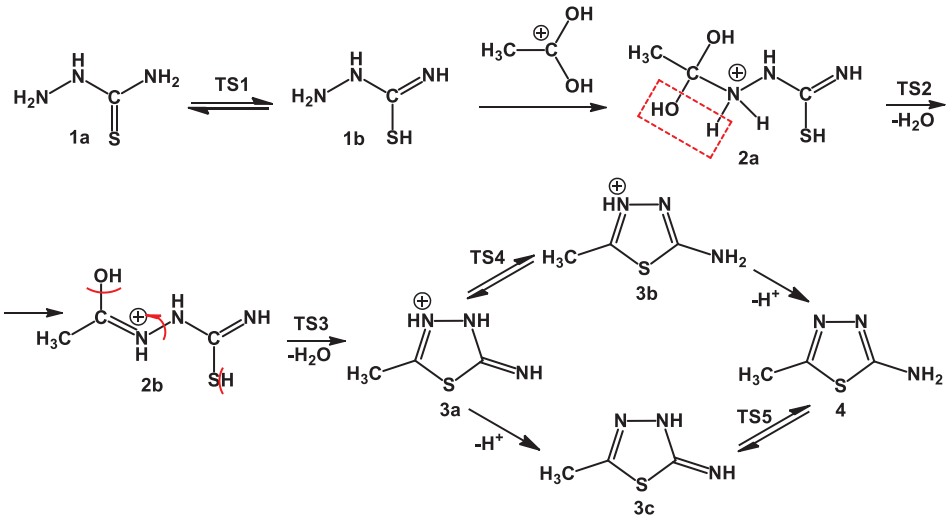

Scheme 1. Probable mechanism of 2-amino-5-methyl-1,3,4-thiadiazole formation.

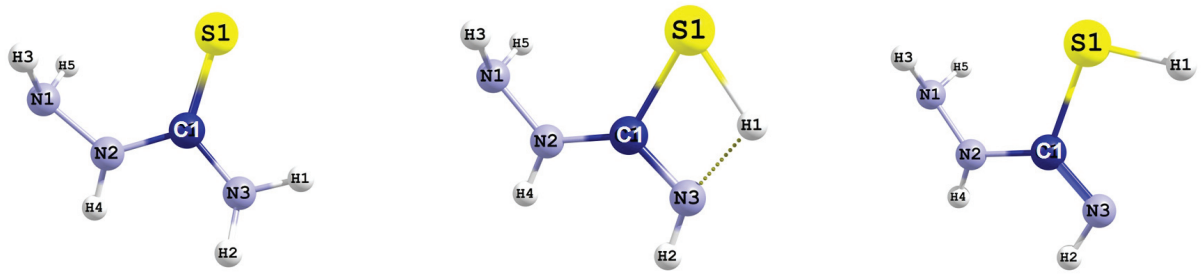

1a **TS1** **1b**

B3LYP/6-31G(d,p)	E_{rel} = 0*	E_{rel} = 41.33	E_{rel} = 19.27
B3LYP/6-311+G(2d2p)	E_{rel} = 0	E_{rel} = 36.42	E_{rel} = 15.35
HF/MP2/6-311+G(2d2p)	E_{rel} = 0	E_{rel} = 53.17	E_{rel} = 19.21

Figure 2. Models, methods and calculated values of relative energy (E_{rel}, kcal·mol^{-1}) of optimized configurations of **1a**, **TS1**, and **1b**. *The total energy of the most stable structure revealed by each method of calculations is assumed as relative energy to be equal to 0.

In pristine molecule **1a** the hydrogen atom H1 is located about 2.756 Å from sulfur atom S1. The distances C1–N3 and C1–S1 are found to be equal to 1.368 Å and 1.679 Å, respectively. The angle N3–C1–S1 is 122.6°. In the transition state **TS1** the N3–C1–S1 angle is decreased to 106.8° and its value approaches to that of tetrahedral angle. On going from **TS1** to **1b** the value of N3–C1–S1 angle is increased slightly to 119.8°, and its value is close to the similar angle of **1a**. The length of C1–N3 bond of **1b** is estimated to be of 1.275 Å and its character is approached to double bond.

The bond lengths and angles in the thiosemicarbazide **1a** calculated by quantum chemical methods are in agreement with the results of X-ray analysis (Table 1).[39]

Since the reaction occurs in the acid medium, the protonation of acetic acid molecules takes place. The interaction of a protonated acetic acid with **1b** leads to **2a** formation (Scheme 3).

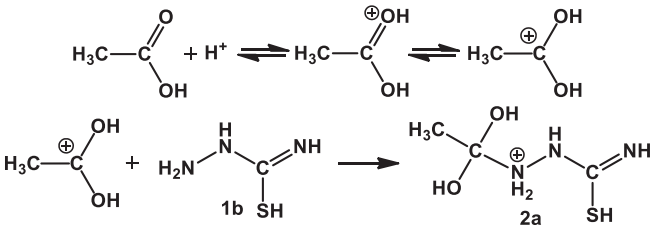

Scheme 3. The protonation of acetic acid and its interaction with **1b**.

The **2b** formation occurs due to dehydratation of **2a** which runs *via* four-central transition state **TS2**. The views of optimized configurations **2a**, **TS2**, and **2b** are shown in Figure 3.

The transition state formation **TS2** occurs due to intramolecular transfer of hydrogen atom H8 from nitrogen atom N1 to oxygen atom O2. Thereby, significant loosening of O2–H8 bond to 1.215 Å is observed, due to hydrogen bond formation.[40] The distance N1–H8 is estimated to be 1.378 Å what is determined by significant hydrogen bond impact. Moreover, comparing with **2a**, length bond C1–O2 of **TS2** is increased from 1.370 Å to 1.536 Å. The relaxation of **TS2** to **2b** leads to significant shortening of the C1–N1 bond length to 1.324 Å, and its character is approached to that of double bond.

The free rotation of the fragments in **2b** around the N1–N2 bond leads to further formation of **3a** through the four-center transition state **TS3**. As a result, the S1 and O1 atoms turn out to be spatially close, the S1–H5 bond is relaxed and a new O1–H5 bond is formed. Subsequent elimination of the water molecule leads to the formation

Table 1. Selected bond lengths and angles for **1a** by quantum chemical calculations and X-ray analysis data.

Selected bond lengths, Å, and angles, °, for **1a**	DFT/B3LYP/6-31G(d,p)	DFT/B3LYP/6-311+G(2d2p)	MP2/6-311+G(2d2p)	X-Ray analysis[39]
C1–N3	1.368	1.368	1.374	1.316
C1–N2	1.365	1.363	1.364	1.327
C1–S1	1.679	1.670	1.655	1.704
N2–N1	1.407	1.407	1.407	1.401
N3–C1–N2	114.04	113.82	112.99	118.56
N3–C1–S1	122.62	122.56	123.37	122.14
N2–C1–S1	123.33	123.60	123.62	119.28
C1–N2–N1	123.38	123.04	121.96	121.40

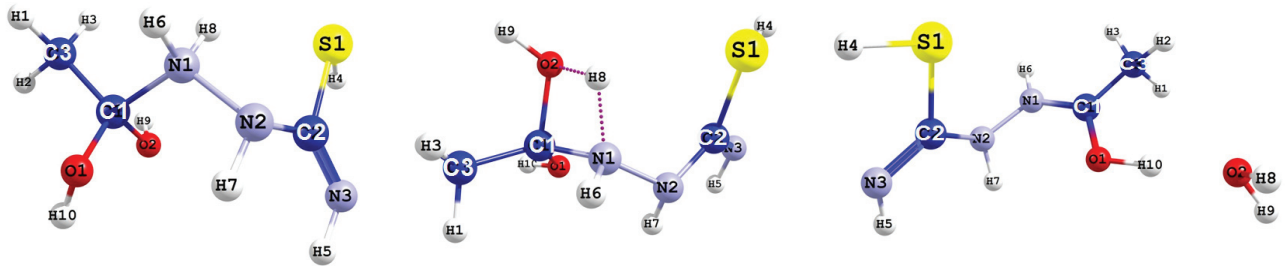

	2a	**TS2**	**2b**
B3LYP/6-31G(d,p)	E_{rel} = 21.79	E_{rel} = 54.94	E_{rel} = 0
B3LYP/6-311+G(2d2p)	E_{rel} = 24.66	E_{rel} = 53.57	E_{rel} = 0
MP2/6-311+G(2d2p)	E_{rel} = 22.76	E_{rel} = 69.43	E_{rel} = 0

Figure 3. Views and calculated values of relative energy (E_{rel}, kcal·mol^{-1}) of the optimized configurations **2a**, **TS2**, and **2b**.

of **3a**. The **2b**, **TS3**, and **3a**-water models optimized using the DFT B3LYP/6-31G(d,p) are shown in Figure 4.

The formation of target **4** can be realized by two ways: 1) tautomeric transformation of **3a**–**3b**, which occurs through the four-center transition state **TS4**, and deprotonation of **3b** or 2) deprotonation of **3a** and tautomerism of **3c**–**4** *via* transition state **TS5** (Scheme 1). Due to present of imino group and hydrogen atoms at intercycle nitrogen atoms, **3a** can form a tautomeric structure **3b** (Scheme 1).

It was established that intramolecular transfer of hydrogen atom H6 between intracyclic nitrogen atom N2 and nitrogen atom of imino group N3 occurs through the four-center transition state **TS4**. Models **3a**, **TS4**, and **3b** optimized are shown in Figure 5.

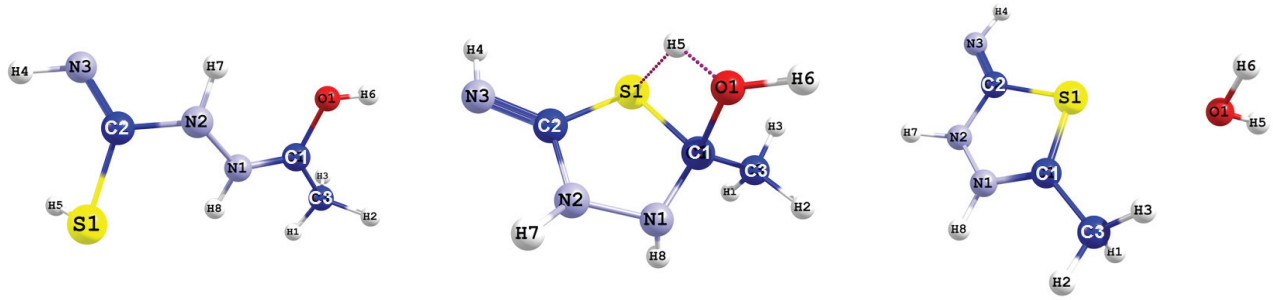

	2b-H_2O	**TS3**	**3a+H_2O**
B3LYP/6-31G(d,p)	E_{rel} = 0.55	E_{rel} = 50.01	E_{rel} = 0
B3LYP/6-311+G(2d2p)	E_{rel} = 9.00	E_{rel} = 50.56	E_{rel} = 0
MP2/6-311+G(2d2p)	E_{rel} = 4.04	E_{rel} = 69.99	E_{rel} = 0

Figure 4. Models and calculated values of relative energy (E_{rel}, kcal·mol^{-1}) of the optimized configurations **2b**, **TS3**, and **3a**.

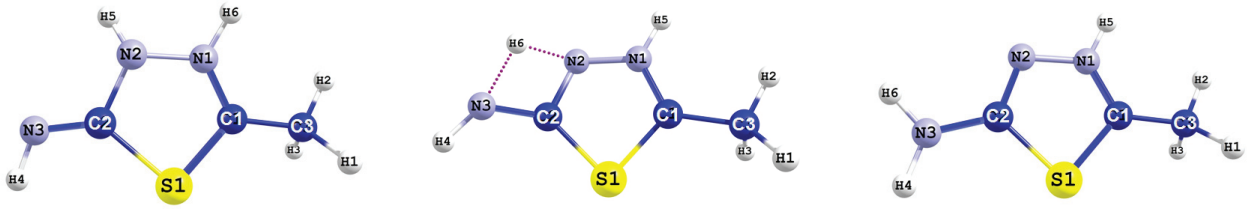

	3a	**TS4**	**3b**
B3LYP/6-31G(d,p)	E_{rel} = 25.08	E_{rel} = 66.12	E_{rel} = 0
B3LYP/6-311+G(2d2p)	E_{rel} = 23.48	E_{rel} = 62.84	E_{rel} = 0
MP2/6-311+G(2d2p)	E_{rel} = 23.35	E_{rel} = 81.55	E_{rel} = 0

Figure 5. Models, methods and calculated values of relative energy (E_{rel}, kcal·mol^{-1}) of the optimized configurations **3a**, **TS4**, and **3b**.

By B3LYP/6-31G(d,p) calculations it was determined that in parent molecule **3a** the hydrogen atom H6 remotes from nitrogen atom N2 at 1.017 Å. The distances C2–N2, C2–N3 and C2–S1 are 1.412 Å, 1.246 Å and 1.854 Å, respectively. The angle N2–C2–N3 is 122.4°. In transition state **TS4** the angle N2–C2–N3 is decreased to 106° and approximates at value by tetrahedral.

In tautomer **3b** the angle N2–C2–N3 is increased to 123.65°, *i.e.* approximates to value of such angle in molecule **3a**. The length bond C2–N2 is 1.316 Å and its character is approached to double bond.[40]

Tautomeric transformation **3c**–**4** occurs *via* transition state **TS5**. Views of **3c**, **TS5** and **4** are shown in Figure 6.

In molecule **3c** the length bond N2–H5 is 1.006 Å. This bond is increased to 1.320 Å in transition state **TS5**. The angle N2–C2–N3 is 123.654° in tautomer **3c**. In transition state **TS5** this angle N2–C2–N3 decreases to 106.16° and approximates at value by tetrahedral. In molecule **4** the angle N2–C2–N3 is increased to 123.52°, *i.e.* approximates to value of such angle in molecule **3b**. Following the results obtained by three applied computation methods, pathway via **TS5** is realized via the higher activation barrier what is considered as less probable if compared with an alternative path via **TS4** (Figure 7).

Atom coordinates of the optimized configuration of **1a**, **TS1**, **1b**, **2a**, **TS2**, **2b**, **TS3**, **3a**, **TS4**, **3b**, **3c**, **TS5**, **4** are collected in Supplementary Materials (Tables S1–S4).

Thus, it was established by quantum chemistry methods that the target 2-amino-5-methyl-1,3,4-thiadiazole formation is complicated multi-stage process which occurs through a number of elementary chemical transformations with overcoming of four activation barriers; cyclic product formation stage has a limitative rate. In a row B3LYP/6-311+G(2d2p) => B3LYP/6-31G(d,p) => MP2/6-311+G(2d2p), the values of activation barriers increase (Figure 7).

Values of enthalpy and Gibbs energy of reactants and products at 298.15 (room temperature) and 393.15 K (temperature of experiment[1]) were evaluated by B3LYP/6-311+G(2d2p) for configurations optimized by B3LYP/6-311+G(2d2p) method are shown in Table 2.

Table 2. Values of enthalpy (H, kcal/mol) and Gibbs free energy (G, kcal/mol) calculated at 298.15 and 373.15 K by B3LYP/6-311+G(2d2p) level for configurations optimized by B3LYP/6-311+G(2d2p).

Compound	298.15 K		373.15 K	
	ΔH	ΔG	ΔH	ΔG
1a	55.43	24.72	55.69	23.89
1b	51.21	28.20	53.11	22.20
2a	102.95	72.29	106.42	64.19
2b	101.81	68.03	105.47	59.12
2b-H2O	84.63	54.68	87.57	46.81
3a+H2O	85.00	54.07	88.15	45.94
3a	67.80	43.01	70.10	36.51
3b	68.18	42.87	70.51	36.24
3c	59.74	35.05	61.95	28.58
4	59.79	35.33	62.00	28.93

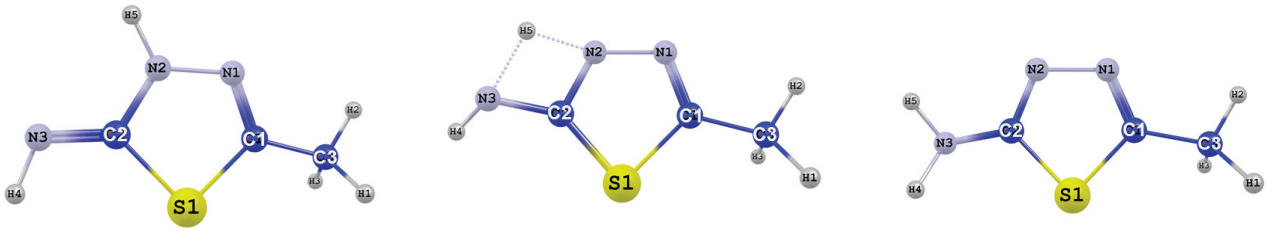

Figure 6. Views and calculated values of relative energy (E_{rel}, kcal·mol^{-1}) of optimized configurations **3c**, **TS5**, and **4**.

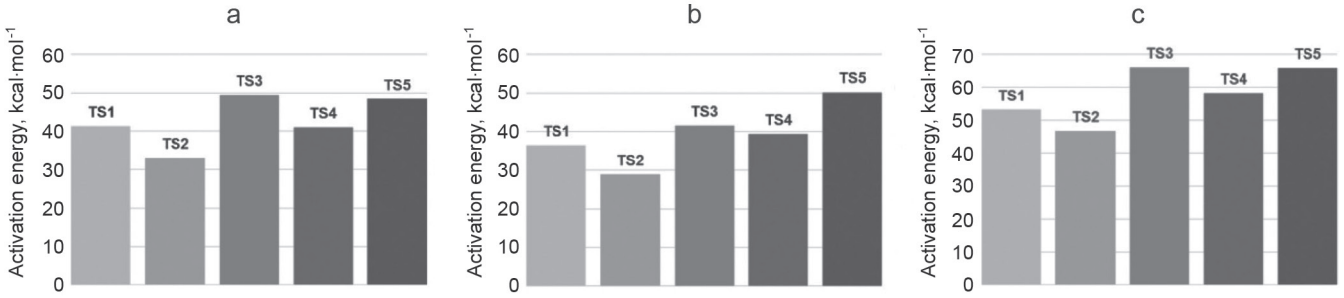

Figure 7. Diagrams of relative activation energy (kcal·mol^{-1}) of tranformations **1a – TS1**, **2a – TS2**, **2b – TS3** and **3a – TS4**. a) B3LYP/6-31G(d,p), b) B3LYP/6-311+G(2d2p), c) MP2/6-311+G(2d2p).

Following the data shown in Table 2 an increasing of the temperature is favorable to shifting the equilibrium processes towards the products.

Conclusions

Multi-stage process of 2-amino-5-methyl-1,3,4-thiadiazole formation was studied by quantum chemistry DFT and MP2 methods with 6-311+G(2d2p) basis sets. Activation barriers of each of the elemental stage were estimated by DFT and MP2 methods. It was shown that the transformation of protonated methyliminothiadiazole **3a** into target compound **4** can be realized by two ways and deprotonation-tautomerism pathway was estimated to be the most favorable. In comparison with DFT, the MP2 method in general overestimates the values of activation barriers. Based on calculation results the most probable mechanism of 2-amino-5-methyl-1,3,4-thiadiazole formation was generated.

Acknowledgments. This study was financially supported by the Russian Foundation for Basic Research (grant no. 19-03-00888).

References

1. Ashutosh B., Ankur J., Kumar N.R., Sonia G., Niharika S., Vivek D., Pramod S. *Int. J. Pharm. Sci. Drug Res.* **2009**, *1*(3), 207.
2. Danilova E.A., Melenchuk T.V., Trukhina O.N., Islyaikin M.K. *Macroheterocycles* **2010**, *3*, 68.
3. Jain A.K., Sharma S., Vaidya A., Ravichandran V., Agrawal R.K. *Chem. Biol. Drug Des.* **2013**, *81*, 557.
4. Danilova E.A., Kudayarova T.V., Islyaikin M.K., Koifman O.I. *Ross. Khim. Zh.* [*Russ. Chem. J.*] **2016**, LX(2), 59.
5. Melenchuk T.V., Danilova E.A., Stryapan M.G., Islyaikin M.K. *Russ. J. Gen. Chem*. **2008**, *78*, 495.
6. Kudrik E.V., Islyaikin M.K., Smirnov R.P. *Russ. J. Gen. Chem.* **1996**, *66*(9), 1564.
7. Danilova E.A., Vorontsova A.A., Melenchuk T.V., Islyaikin M.K., Ananieva G.A., Bykova V.V., Usol'tseva N.V. *Liquid Crystals and their Application* **2011**, (1), 17.
8. Filatov M.S., Kudayarova T.V., Danilova E.A., Islyaikin M.K. *ChemChemTech [Izv. Vyssh. Uchebn. Zaved., Khim. Khim. Tekhnol.]* **2014**, *57*(7), 21.
9. Danilova E.A., Butina Yu.V., Kudayarova T.V., Islyaikin M.K.. *ChemChemTech [Izv. Vyssh. Uchebn. Zaved., Khim. Khim. Tekhnol.]* **2014**, *57*(10), 20.
10. Kudayarova T.V., Danilova E.A., Islyaikin M.K. *ChemChemTech [Izv. Vyssh. Uchebn. Zaved., Khim. Khim. Tekhnol.]* **2015**, *58*(11), 16.
11. Sessler J.L., Miller R.A. *Biochem. Pharmacol*. **2000**, *59*, 733.
12. Sessler J.L., Seidel D. *Angew. Chem. Int. Ed.* **2003**, *42*, 5134.
13. Yoon Z.S., Kwon J.H., Yoon M., Koh M.K., Noh S.B., Sessler J.L., Lee J.T., Seidel D., Aguilar A., Shimizu S., Suzuki M., Osuka A., Kim D. *J. Am. Chem. Soc*. **2006**, *128*, 14128.
14. Sessler J.L., Gale P.A., Cho W.S. *Anion Receptor Chemistry* (Stoddart J.F., Ed.). Cambridge: Royal Society of Chemistry, **2006**.
15. Ghosh S.K., Ishida M., Cha J.L.W., Lynch V.M., Kim D., Sessler J.L. *Chem. Commun*. **2014**, *50*, 3753.
16. Kataev E.A., Pantos P., Karnas E., Kolesnikov G.V., Tananaev I.G., Lynch V.M., Sessler J.L. *Supramol. Chem.* **2015**, *27*, 346.
17. He Q., Tu P., Sessler J.L. *Chem*. **2018**, *4*(1), 46.
18. Wagner-Wysiecka E.,· Łukasik N., Biernat J.F., Luboch E. *J. Inclusion Phenom. Macrocycl. Chem.* **2018**, *90*, 189.
19. Lindeman S.V., Shklover V.E., Struchkov Yu.T., Ponomarev I.I., Siling S.A., Vinogradova S.V., Korshak V.V. *Izv. AN SSSR* **1984**, 2015.
20. Kudrik E.V., Islyaikin M.K., Smirnov R.P., Kuz'michenko A.V. Patent RF 2134270, **1999**.
21. Eckert A.K., Trukhina O.N., Rodríguez-Morgade M.S., Danilova E.A., Islyaikin M.K., Torres T. *Mendeleev Commun.* **2010**, *20*(4), 192.
22. Butina Yu.V., Danilova E.A., Kudayarova T.V. *Macroheterocycles* **2016**, *9*, 206.
23. Kobayashi N. *ChemChemTech [Izv. Vyssh. Uchebn. Zaved. Khim. Khim. Tekhnol.]* **2019**, *62*(8), 4–25.
24. Shreve R.N., Charlesworth R.K. Patent USA 2744116, 1956.
25. Barmin M.I.. *ChemChemTech [Izv. Vyssh. Uchebn. Zaved., Khim. Khim. Tekhnol.]* **2005**, *48*(9), 103.
26. Julia M.S., Sala P., Mazo J. *J. Heterocycl. Chem*. **1982**, *19*(5), 1141.
27. Torres J., Lavandera J.L., Cabildo P., Claramunt R.M., J. Elguero. *J. Heterocyclic Chem*. **1968**, *5*(6), 771.
28. Hu Y., Li C.Y., Wang X.M., Yang Y.H., Zhu H.L. *Chem. Rev.*, **2014**, *114*, 5572.
29. Butina Yu.V., Danilova E.A., Islyaikin M.K. In: *Quantum-Chemical Calculations: Structure and Reactivity of Organic and Inorganic Molecules*. Ivanovo, **2017**. p. 96–100.
30. Mashaly M.M. *Synth. React. Inorg. Met.-Org. Chem.* **2002**, *32*(2), 373.
31. Granovsky A.A.. Firefly version 8. *http://classic.chem.msu.su/gran/firefly/index.html*.
32. Schmidt M.W., Baldridge K.K., Boatz J.A., Elbert S.T., Gordon M.S., Jensen J.H., Koseki S., Matsunaga N., Nguyen K.A., Su S., Windus T.L., Dupuis M., Montgomery J.A. *J. Comput. Chem*. **1993**, *14*, 1347–1363.
33. Tsirelson V.G. *Quantum Chemistry. Molecules, Molecular Systems and Solids*. Moscow: Binom, **2010**.
34. Andrienko G.A.. ChemCraft version 1.8, build 428. *http://www.chemcraftprog.com/index.html*.
35. Galabov B., Nalbantova D., von R. Schleyer P., Schaefer H.F. *Acc. Chem. Res.* **2016**, *49*, 1191–1199.
36. Galabov B., Koleva G., Simova S., Hadjieva B., Schaefer H.F., von R. Schleyer P. *PNAS* **2014**, *111*(28).
37. Koleva G., Galabov B., Kong J., Schaefer H.F., von R. Schleyer P. *J. Am. Chem. Soc.* **2011**, *133*, 19094–19101.
38. Pavlyuchko A.I., Vasiliev E.V., Gribov L.A. *J. Struct. Chem*. **2012**, *53*, 278.
39. Srinivasan B.R., Raghavaiah P., Nadkarni V.S. *Spectrochim. Acta, Part A: Molecular and Biomolecular Spectroscopy* **2013**, 112, 84–89.
40. *Chemical Encyclopedia*, Vol. 2 (Knunyants I.L., Ed.), Moscow: Sov. encycl., **1990**.

Received 16.12.2021
Accepted 17.01.2022